

Evaluation of Piezoresistivity Properties of Sputtered ZnO Thin Films

Guilherme Wellington Alves Cardoso^{a*}, Gabriela Leal^a, Argemiro Soares da Silva Sobrinho^a,

Mariana Amorim Fraga^b, Marcos Massi^{a,c}

^aInstituto Tecnológico de Aeronáutica – ITA, São José dos Campos, SP, Brasil

^bFaculdade de Tecnologia de São Paulo – FATEC-SP, São Paulo, SP, Brasil

^cUniversidade Federal de São Paulo – UNIFESP, São José dos Campos, SP, Brasil

Received: June 6, 2013; Revised: April 22, 2014

Zinc oxide (ZnO) thin films were deposited by RF reactive magnetron sputtering on silicon (100) substrates under different experimental conditions. ZnO films were studied before and after annealing treatment at 600 °C. The crystallinity, electrical resistivity, stoichiometry, thickness, and elastic modulus of the films were investigated. ZnO piezoresistors were produced using microelectronics processes, such as photolithography, lift-off, and reactive ion etching (RIE). Cantilever method was used to determine the gauge factor, and measurements of Temperature Coefficient of Resistance (TCR) were performed on a hotplate. The optimization of the deposition conditions produced ZnO thin films with controlled stoichiometry (ZnO), crystalline microstructure (phase wurzite, 002), high elastic modulus (156 GPa), and low electrical resistivity (0.072 ohm.cm), which are good properties for application as piezoresistive pressure microsensors. In addition, the ZnO piezoresistors had a GF of 2.6 on the deformation in the plane (100) and TCR of -1610 ppm/K up to 250 °C.

Keywords: ZnO, thin film, magnetron sputtering, piezoresistivity

1. Introduction

Zinc oxide (ZnO) thin films have been used in the fabrication of electronics devices such as diodes¹, thin films transistors (TFTs)², and Micro-Electro-Mechanical System (MEMS) such as gas sensors³. ZnO is a wide band gap (3.37 eV) semiconductor material with thermal and chemical stabilities. The combination of these properties with the outstanding piezoelectric characteristics make this material a potential candidate to replace silicon in MEMS sensors employed in hostile environments, i.e. at high temperatures.

The literature mostly presents works related to piezoresistive properties of high band gap materials such as silicon carbide (SiC) and diamond. On the other hand, few studies report the piezoresistive characteristics of ZnO. This may be attributed to the following reasons: (a) the piezoelectric properties of ZnO are well documented in the literature⁴⁻⁶; (b) compared to SiC⁷ and diamond, ZnO exhibits lower electromechanical properties.

Despite the lower electromechanical characteristics when compared to other semiconductor materials, ZnO may have advantages because its crystallographic structure is well defined⁸. The ordered crystallographic configuration of ZnO is related to the substrate type and deposition parameters employed during its formation. On the other hand, SiC has more than 200 polytypes with different physical properties⁹, and the highly ordered atomic structure of diamond inhibits doping processes necessary to reduce its resistivity.

The ability to change electrical resistivity when submitted to mechanical stress is known as the piezoresistive

effect, which depends on the doping concentration, crystallographic orientation, and temperature¹⁰. The piezoresistive effect can be determined by a Gauge Factor (GF), which shows the variation of electrical resistance and strain according to Equation 1.

$$GF = \frac{\Delta R}{R} \cdot \frac{1}{\epsilon} \quad (1)$$

Where ΔR is the variation of electrical resistance and ϵ is the strain.

Monocrystalline P type silicon has higher GF (around 140) at room temperature. However, at temperatures higher than 125 °C, this factor is significantly reduced. SiC piezoresistors can exhibit GF in the range of 8 to 50 and thermal stability up to 500 °C according to their crystalline structure¹¹. For these reasons, ZnO is considered as an alternative material in piezoresistive devices due to its thermal stability, which is similar to SiC, ease of synthesis, and well controlled deposition parameters.

Cold plasma assisted techniques have been extensively used to grown these films, because at low temperatures, damage to the previously processed devices are avoided. Among these techniques, Physical Vapor Deposition (PVD) is the most used¹².

2. Experimental

2.1. Samples

RF magnetron sputtering technique was used to deposit ZnO thin films on Si (100) p-type substrates with resistivity

*e-mail: guilherme_wa@hotmail.com

about 1-10 Ω .cm. The silicon substrates were previously cleaned with a solution of $H_2SO_4 - H_2O_2$ (4:1) and then with $H_2O - HF$ (20:1). In order to remove the target oxide layer, 10 min of a pre-sputtering in argon atmosphere was done. Zinc oxide target (99.99 %) located at 75 mm from the substrate was used as cathode target. The deposition time of 60 min and the total gas flow of 20 sccm (19sccm Ar and 1sccm O_2) were kept constant. Table 1 summarizes the varied parameters used in the ZnO deposition processes.

Each sample was divided into two similar pieces. One of them was annealed at 600 °C with heating rate of 20 °C/min at $8.0 \cdot 10^{-3}$ Torr for 60 min. The samples were kept inside the oven until completely cooled.

2.2. Analysis

The thin-film resistivity and crystallinity were characterized using the four point probe technique (Jandel RM3 with 4 points probes) and X-ray diffraction technique (Shimadzu, model XRD-6000, Cu-K α , $\lambda=1.54 \text{ \AA}$), respectively. The film thicknesses were determined using a profilometer (Tencor Instruments Alpha-Step 500). The film compositions were investigated by Rutherford Backscattering Spectroscopy (RBS), and the spectra analyzed using the RUMP simulation code.

The elastic modulus of the ZnO films was obtained by nanoindentation (Hysitron Triboindenter 900). Piezoresistors were fabricated by lithographic process (Figure 1) and characterized by the cantilever method (Figure 2). This process consists of a cantilever with a fixed extremity, where the piezoresistor is placed, and a free extremity, where a calibrated mass is placed, which causes mechanical stress in the piezoresistor. The piezoresistor resistance was measured without mechanical stress (R_0) and with mechanical stress (R_p), caused by a mass placed in the free

cantilever extremity (R_p). Equation 2 was used to determine the resistance variation ($\Delta R/R$).

$$\frac{\Delta R}{R} = \frac{R_f - R_0}{R_0} \quad (2)$$

3. Results and Discussions

Figure 3 shows the deposition rates of the films as a function of applied power and work pressure. The increase of applied power provides an increase in deposition rate of the films as expected. An increase in deposition rate decreased the work pressure¹³. This phenomenon is related to the increase of the sputtered particles arriving in the substrate at lower pressures.

Figure 4 shows the X-ray diffraction spectra of ZnO thin films. Samples 4, 5, and 6, (obtained at higher working pressures) have peaks at 34.4° (002 - wurzite phase), which are smaller and more extended than those obtained for samples 1, 2, and 3, indicating a more disorganized structure, and therefore, less crystalline. At low pressure, the particles produced a substrate with higher values of energy and can form zinc silicate (Zn_2SiO_4) film in the interface, with peak at 25.3° (220)¹⁴.

In addition to the influence of work pressure on the crystallinity of the film, the diffraction patterns also show the influence of the applied power on the film characteristics. As previously mentioned, the sample deposited at higher pressure and lower power (sample 4) has low intensity peaks, and inversely, samples deposited at 5 mTorr and higher power have higher crystallinity. The peak centered at 33.2° refers to silicon substrate.

Four-point probe measurements were performed on all samples, and only samples 2 and 3 had low resistivity, 0.072 and 0.351 Ω .cm, respectively. The other samples showed resistivity out of the 4-point probe scale ($0.5 \cdot 10^9 \Omega/\square$).

Based on these results, samples 2 and 3 had lower resistivity and good crystallinity and were selected to analyze their piezoresistive behavior. Therefore, these two samples were annealed at 600 °C, and the X-ray diffraction patterns are performed (Figure 5). After the annealing process, the samples showed well defined peaks centered at 34.6°. The films are also free of stress, because they possess the central peak equal to the XRD pattern for the ZnO in wurzite phase to the plane 002. Furthermore, the amorphous band (at approximately 30 degrees) disappeared after annealing and the peak of 25.3° (Zn_2SiO_4) decreased,

Table 1. Deposition parameters.

Sample	Discharge Power (W)	Working pressure (mTorr)
1	100	5
2	150	5
3	200	5
4	100	15
5	150	15
6	200	15

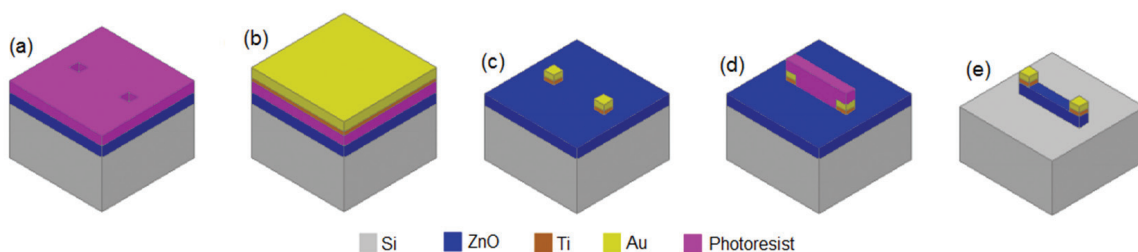


Figure 1. Schematic drawing of the manufacturing process of the resistors, in a) photoresist deposition on ZnO thin film and contact lithography; b) Ti and Au deposition on photoresist to contacts; c) lift-off to contact formation; d) photoresist deposition and resistor lithography; e) RIE to resistor formation.

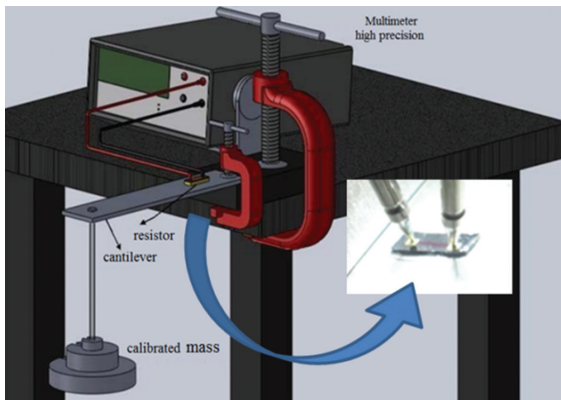


Figure 2. Schematic illustration of the experimental set-up used to characterize the piezoresistors.

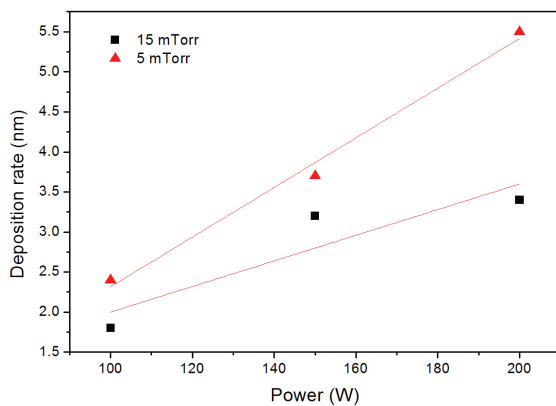


Figure 3. Deposition rate of the ZnO thin films.

which was a further indication that the material had higher crystallinity in wurzite phase.

RBS analysis showed the stoichiometric relation of the Zn and O atoms, independent of the work pressure or power applied. The contaminant presence is insignificant. Figure 6 shows the obtained and simulated spectrum of the sample 3R.

The resistivity of the films before and after annealing process is presented in Table 2. The resistivity of the non-annealed samples is slightly lower than the annealed one.

The resistivity of a material is linked to the organization of its crystal lattice, and as illustrated by X-ray diffraction patterns, the films had higher crystallinity after thermal annealing, which directly reflects the values of resistivity¹⁵. However, if any contaminant contributes to doping, the resistance can vary to higher or lower values¹⁶.

Nanoindentation results of samples 2 and 3 before and after annealing are presented in Figure 7. The annealed samples showed higher elastic modulus than the non-annealed ones. Sample 2R, for example, had an elastic modulus of 156 GPa, which is in accordance with the literature. Annealed films with higher modulus of elasticity values are better for the fabrication of piezoresistive sensors. Therefore, samples 2R and 3R were selected to produce piezoresistors via photolithographic process.

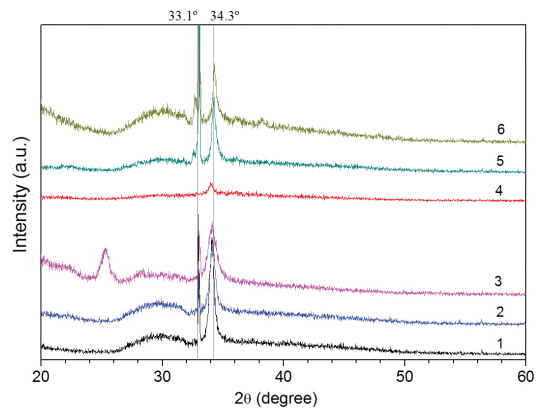


Figure 4. X-ray diffraction of the deposited films.

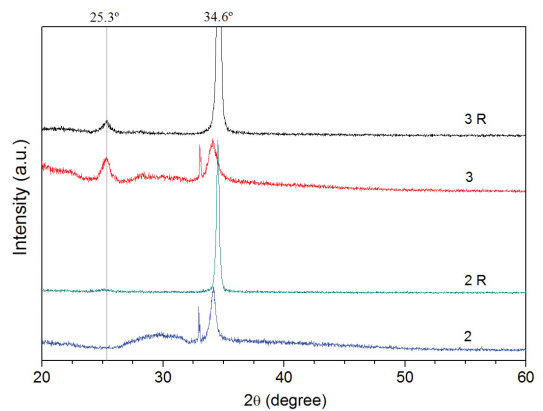


Figure 5. X-ray diffraction of samples before (2 and 3) and after (2R and 3R) annealing.

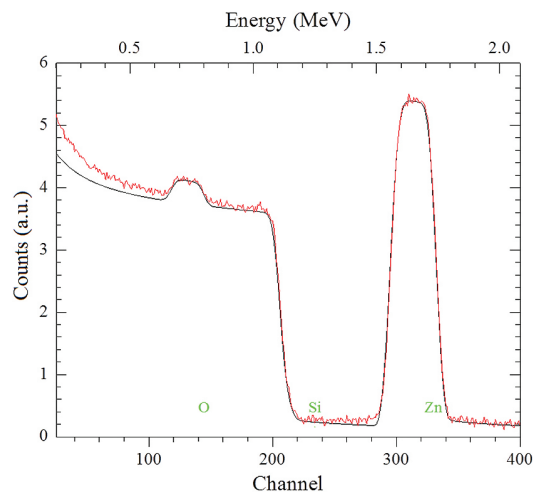


Figure 6. Real and simulated RBS spectrum of sample 2R.

Table 2. Resistivity of the films before and after the annealing.

Samples	Resistivity ($\Omega \cdot \text{cm}$)
2	0.072
2 R	0.074
3	0.351
3 R	1.855

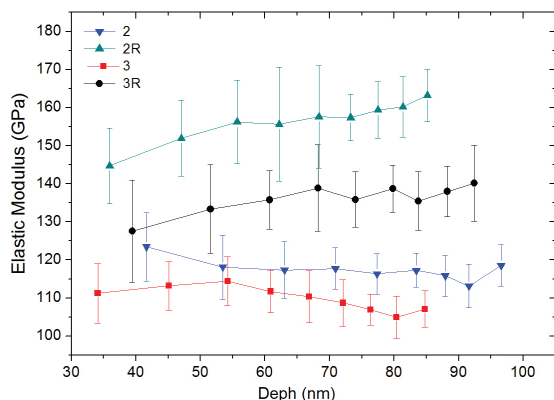


Figure 7. Elastic modulus of ZnO films.

The variation of the resistance as function of the mass applied is shown in Figure 8. Sample 2R had higher elastic modulus, lower resistivity, and a smaller thickness, and it also achieved greater sensitivity to deformation. Low gauge factor of approximately 2.6 ± 0.2 for sample 2R and 1.00 ± 0.05 for 3R was found.

The resistors 2R and 3R were characterized according to temperature coefficient of resistance (TCR), as shown in Figure 9. Sample 2R showed a small variation of resistance compared to sample 3R; even with less thickness, sample 2R is more thermally stable.

The ZnO films had an almost constant TCR up to 525 K. A huge variation occurred above this temperature, suggesting that the morphological structure can have lattice parameter distortion, which can generate resistance variation and affect the use of this material as a pressure sensor above this temperature.

4. Conclusion

From the results obtained in this work, it is possible to conclude that the annealed samples 2 and 3 showed the best piezoresistivity characteristics due to their high elastic modulus and low resistivity. Both films had thermal stability up to 525 K, and sample 2R had high sensitivity to deformation. Future works will be developed using ZnO

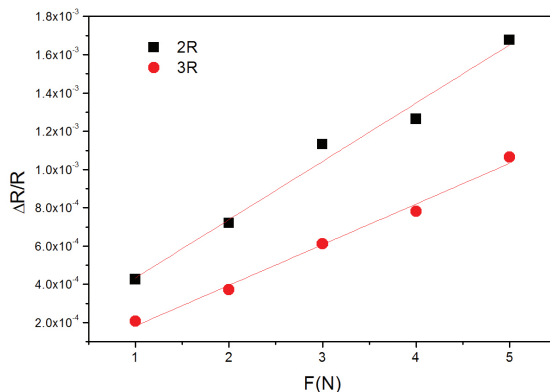


Figure 8. Relative change in resistance ($\Delta R/R$) of the resistors as a function of the applied load on cantilever at room temperature.

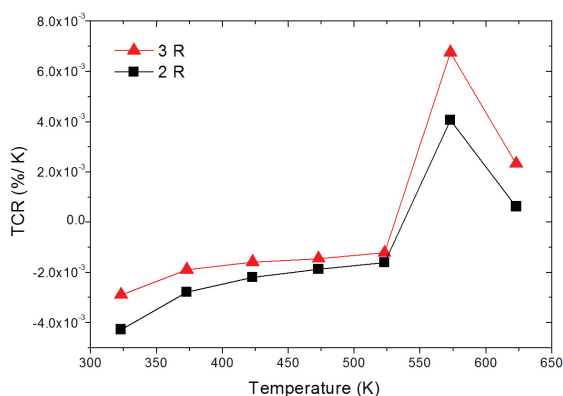


Figure 9. TCR of ZnO films.

doped with titanium (Ti), aluminum (Al), and molybdenum (Mo) to modify its net parameters and thus reduce the film resistivity in order to increase the piezoresistivity capacity.

Acknowledgments

We are thankful to LAS-INPE, LAMFI-IF-USP, LNNano-LNLS, and IP&D-UNIVAP laboratories for the use of characterization equipment and CNPq, CAPES, and FAPESP for the financial support.

References

- Lee SY, Shim ES, Kang HS, Pang SS and Kang JS. Fabrication of ZnO thin film diode using laser annealing. *Thin Solid Films*. 2005; 473(1):31-34. <http://dx.doi.org/10.1016/j.tsf.2004.06.194>
- Lee K, Choi JM, Hwang DK, Oh MS, Kim JK, Jung Y et al. Top-gate ZnO thin-film transistors with a polymer dielectric designed for ultraviolet optical gating. *Sensors and Actuators A: Physical*. 2008; 144(1):69-73. <http://dx.doi.org/10.1016/j.sna.2008.01.012>
- Al-Hardan NH, Abdullah MJ and Aziz AA. Sensing mechanism of hydrogen gas sensor based on RF-sputtered ZnO thin films. *International Journal of Hydrogen Energy*. 2010; 35(9):4428-4434. <http://dx.doi.org/10.1016/j.ijhydene.2010.02.006>
- Mitsuyu T, Ono S and Wasa K. Structures and SAW properties of rf-sputtered single-crystal films of ZnO on sapphire. *Journal of Applied Physics*. 1980; 51(5):2464-2470. <http://dx.doi.org/10.1063/1.328019>
- Tang IT, Wang YC, Hwang WC, Hwang CC, Wu NC, Hwang MP et al. Investigation of piezoelectric ZnO film deposited on diamond like carbon coated onto Si substrate under different sputtering conditions. *Journal of Crystal Growth*. 2003; 252(1-3):190-198. [http://dx.doi.org/10.1016/S0022-0248\(02\)02496-X](http://dx.doi.org/10.1016/S0022-0248(02)02496-X)
- Kang SJ and Joung YH. Influence of substrate temperature on the optical and piezoelectric properties of ZnO thin

- films deposited by rf magnetron sputtering. *Applied Surface Science*. 2007; 253(17):7330-7335. <http://dx.doi.org/10.1016/j.apsusc.2007.03.020>
7. Fraga MA, Furlan H, Massi M, Oliveira IC and Koberstein LL. Fabrication and characterization of a View the MathML source piezoresistive pressure sensor. *Procedia Engineering*. 2010; 5:609-6012. <http://dx.doi.org/10.1016/j.proeng.2010.09.183>
 8. Sundaram KB and Khan A. Characterization and optimization of zinc oxide films by r.f. magnetron sputtering. *Thin Solid Films*. 1997; 295(1-2):87-91. [http://dx.doi.org/10.1016/S0040-6090\(96\)09274-7](http://dx.doi.org/10.1016/S0040-6090(96)09274-7)
 9. Robert JL, Contreras S, Camassel J, Pernot J, Neyret E, Cioccio L et al. 4H-SiC: a material for high temperature Hall sensor. *Sensors and Actuators A*. 2002; 97-98:27-32. [http://dx.doi.org/10.1016/S0924-4247\(01\)00812-3](http://dx.doi.org/10.1016/S0924-4247(01)00812-3)
 10. Strass J, Eickhoff M and Kroetz G. The influence of crystal quality on the piezoresistive effect of β -SiC between RT and 450°C measured by using microstructures. In: *International Solid State Sensors and Actuators Conference (Transducers '97)*; 1997; Chicago. Volume 2. <http://dx.doi.org/10.1109/SENSOR.1997.635735>
 11. Cocuzza M. Development of Silicon Carbide-Based Micro-Electromechanical Systems. [Thesis]. Trento: Università di Trento; 2006.
 12. Madou MJ. *Fundamentals of microfabrication: the science of miniaturization*. Boca Raton: CRC Press; 2002. p. 144-152.
 13. Gao W and Li Z. ZnO thin films produced by magnetron sputtering. *Ceramics International*. 2004; 30(7):1155-1159. <http://dx.doi.org/10.1016/j.ceramint.2003.12.197>
 14. Wang WC, Tian YT, Li K, Lu EY, Gong DS and Li XJ. Capacitive humidity-sensing properties of Zn₂SiO₄ film grown on silicon nanoporous pillar array. *Applied Surface Science*. 2013; 273:372-376. <http://dx.doi.org/10.1016/j.apsusc.2013.02.045>
 15. Kim KS, Kim HW and Kim NH. *Physica B: Condensed Matter*. 2003; 334(3-4):343-346. [http://dx.doi.org/10.1016/S0921-4526\(03\)00096-6](http://dx.doi.org/10.1016/S0921-4526(03)00096-6)
 16. Wenas WW, Yamada A, Takahashi K, Yoshino M and Konagai M. Electrical and optical properties of boron-doped ZnO thin films for solar cells grown by metalorganic chemical vapor deposition. *Journal of Applied Physics*. 1991; 70:7119-7123. <http://dx.doi.org/10.1063/1.349794>